Presynaptic NR2A-containing NMDA receptors implement a high-pass filter synaptic plasticity rule

Céline Bidoret, Annick Ayon, Boris Barbour, and Mariano Casado[1]

Laboratoire de Neurobiologie, Ecole Normale Supérieure, Centre National de la Recherche Scientifique, 46 rue d'Ulm, 75005 Paris, France

Edited by Charles F. Stevens, The Salk Institute for Biological Studies, La Jolla, CA, and approved June 30, 2009 (received for review April 20, 2009)

The detailed characterization of synaptic plasticity has led to the replacement of simple Hebbian rules by more complex rules depending on the order of presynaptic and postsynaptic action potentials. Here, we describe a mechanism endowing a plasticity rule with additional computational complexity—a dependence on the pattern of presynaptic action potentials. The classical Hebbian rule is based on detection of conjunctive presynaptic and postsynaptic activity by postsynaptic NMDA receptors, but there is also accumulating evidence for the existence of presynaptic NMDA receptors in several brain structures. Here, we examine the role of presynaptic NMDA receptors in defining the temporal structure of the plasticity rule governing induction of long-term depression (LTD) at the cerebellar parallel fiber-Purkinje cell synapse. We show that multiple presynaptic action potentials at frequencies between 40 Hz and 1 kHz are necessary for LTD induction. We characterize the subtype, kinetics, and role of presynaptic NMDA receptors involved in the induction of LTD, showing how the kinetics of the NR2A subunits expressed by parallel fibers implement a high-pass filter plasticity rule that will selectively attenuate synapses undergoing high-frequency bursts of activity. Depending on the type of NMDA receptor subunit expressed, high-pass filters of different corner frequencies could be implemented at other synapses expressing NMDA autoreceptors.

autoreceptors | cerebellum | LTD

Computation in the nervous system emerges from signal integration. This may be achieved at global, network, cellular, synaptic, and finally molecular levels. Synapses may undergo long-term increases or decreases in synaptic strength depending on differences in the patterns of neural activity. How synaptic elements detect those patterns and translate them into synaptic modifications has been a central issue in neuroscience research. Glutamate receptors of the NMDA type are often seen as molecular coincidence detectors, a role arising from their biophysical properties. In addition to gating by glutamate, conduction by NMDA channels requires membrane depolarization to relieve the voltage-dependent Mg block (1, 2). NMDA receptors (NMDARs) located on the postsynaptic elements translate these biophysical requirements into computational coincidence between presynaptic activity, releasing the agonist and postsynaptic depolarization allowing Mg unblock. In these conditions, NMDAR activation is a key step in the induction of several forms of synaptic plasticity.

The study of the role of NMDARs in plasticity has concentrated on postsynaptic NMDARs. However, accumulating evidence suggests the existence of NMDAR located on presynaptic elements in cortex, spinal cord, hippocampus, and cerebellum. Presynaptic NMDARs may be present at both glutamatergic (3–9) and GABAergic terminals (10–13). The activation of presynaptic NMDAR has been shown to be required for long-term plasticity in diverse structures (8, 9, 12, 14; for a review, see 15). However, the role of presynaptic NMDARs in defining plasticity rules remains unclear.

We have shown that NMDARs are required for long-term depression (LTD) of the AMPA-receptor-mediated glutamatergic synaptic transmission between granule cells (GC) and Purkinje cells (PC) in the cerebellar cortex (14). Cerebellar LTD is produced when parallel fiber (PF, granule cell axon) activity is coupled with climbing fiber activity (16). The molecular events associated with LTD induction and expression have been extensively studied. LTD expression has been shown to be postsynaptic, being associated with a reduction in AMPA receptor number (17). Triggering of AMPA receptor endocytosis depends on an elaborate balance between phosphorylation and dephosphorylation of receptors and receptor-associated proteins (17, 18). Two main signaling pathways modify this balance: first, Ca rises in the PC elicited by climbing fiber activity (19) and, second, transcellular NO signaling after PF activity (20–24). We have proposed that NO production arises from the activation of NMDARs located on PFs (see *Discussion*) (14, 24). LTD induction depends on high-frequency repetitive activity of PFs. By combining immunohistochemistry, pharmacological studies of LTD induction in cerebellar slices and recordings from recombinant NMDARs expressed in heterologous cells, we show that the frequency dependence of LTD arises from the activation of NMDARs on PFs. We demonstrate that the NMDARs involved in LTD contain the NR2A subunit. The deactivation kinetics of NR2A-containing NMDARs determines the high frequencies of activity required for LTD induction. The kinetic properties of presynaptic NMDARs therefore explain the precise activity patterns selected by the plasticity induction rule.

Results

High-Frequency PF Activity Is Required for LTD Induction. LTD of PF-PC synapses was induced by a protocol pairing PC depolarization with a doublet of PF stimulations (at 1 Hz for 2 min) (Fig. 1*A*) (14). A protocol with 5-ms interval between the PF stimuli resulted in a robust LTD (EPSC depression 30 min after pairing: 34.7 ± 6.2%; $n = 9$, $P < 0.005$). In contrast, an induction protocol consisting of single PF stimulations failed to induce LTD (−1.8 ± 5.8%, $n = 6$, $P = 1$) (Fig. 1*B*). Thus, synapses that undergo repetitive activity are selectively depressed.

In vivo, PFs are known to fire both tonically and in bursts of diverse frequencies up to at least 1 kHz (25, 26). We studied the magnitude of LTD over a range of physiologically relevant PF frequencies (Fig. 1*C*). Of the intervals tested, 1 and 5 ms were the most effective for depressing the synapses (32.3 ± 5.7%, $n = 8$, $P < 0.01$ and 34.7 ± 6.2%, $n = 9$, $P < 0.005$ of the control value, respectively). A 15-ms interval was still able to induce LTD (30.1 ± 8.6%, $n = 5$, $P = 0.06$). However, a 30-ms interval was only effective in a few cells (13.4 ± 11.2%, $n = 6$, $P = 0.69$). A 60-ms interval was ineffective for inducing LTD (6.6 ± 4.2%, $n = 4$, $P = 0.63$). Similar results were obtained with protocols intended to be closer to physiological conditions, i.e., by replacing the PC depolarization by climbing fiber stimulation (Fig. S1), or when more sparse PF stimulation was carried out by stimulating in the granule cell layer

Author contributions: C.B., B.B., and M.C. designed research; C.B., A.A., B.B., and M.C. performed research; C.B. and M.C. analyzed data; and C.B., B.B., and M.C. wrote the paper.

The authors declare no conflict of interest.

This article is a PNAS Direct Submission.

[1]To whom correspondence should be addressed. E-mail: casado@biologie.ens.fr.

This article contains supporting information online at www.pnas.org/cgi/content/full/0904284106/DCSupplemental.

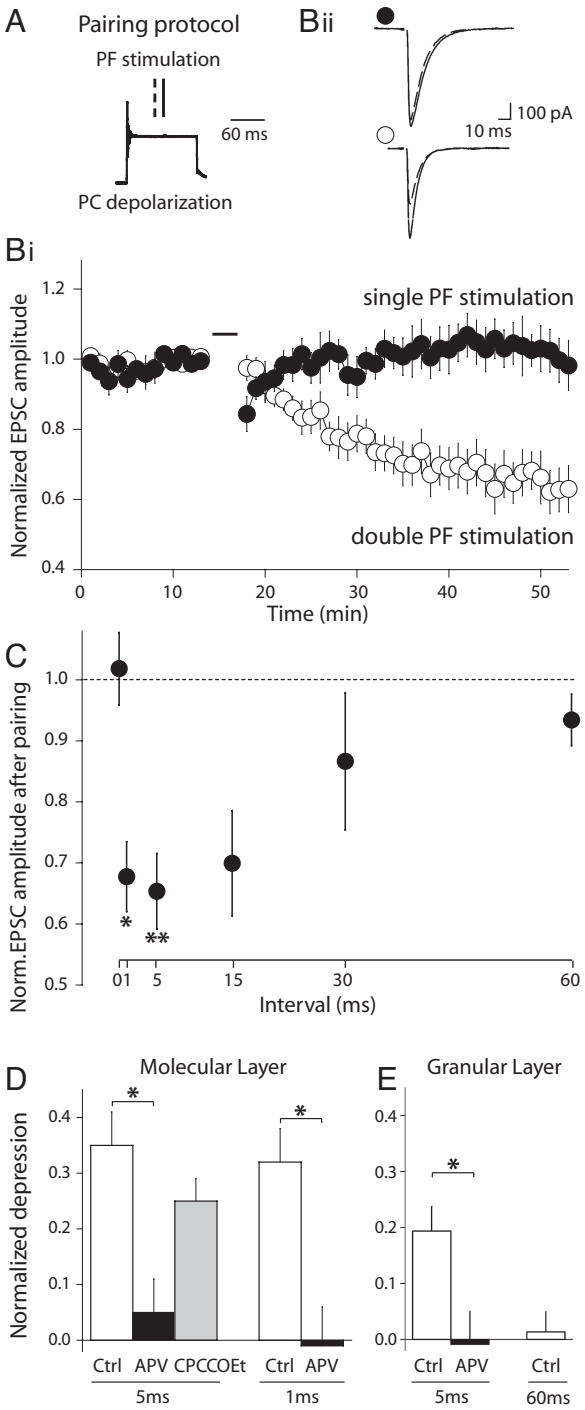

Fig. 1. LTD induction requires high-frequency PF activity and NMDAR activation. (*A* and *B*) LTD was induced only when PFs fired at least twice. (*A*) LTD induction protocol consisted of pairing (at 1 Hz for 2 min) a PC depolarization with a double PF stimulation. The second PF stimulus (solid line) was applied at the middle of the PC depolarization whereas the position of the first (dashed line) varied. (*Bi*) Time course of the normalized EPSC amplitude in experiments where pairing was done with single (black; $n = 6$) or double PF stimuli at a 5-ms interval (white; $n = 9$). (*Bii*) Representative recordings from the experiments in *Bi*. The PF stimulation during the pairing protocol consisted of single PF stimuli (*Upper*) or double PF stimuli at a 5-ms interval (*Lower*). Traces are averages of 10 sweeps, before pairing (solid) and 30 min after pairing (dashed). (*C*) The magnitude of LTD depends on the interval between the two PF stimuli. Normalized EPSC amplitude after pairing with single PF stimulus (0-ms interval, $n = 6$), or with double PF stimuli at intervals of: 1 ms ($n = 8$), 5 ms ($n = 9$), 15 ms ($n = 5$), 30 ms ($n = 6$), or 60 ms ($n = 4$). Asterisks indicate statistical significance of the depression magnitudes. *, $P < 0.01$; **, $P < 0.005$; Sign test. (*D*) NMDARs but not mGluR1s are required for LTD induction. LTD is prevented by D-APV but not by CPCCOEt. Depression induced by pairing with double PF stimuli at 5-ms and at 1-ms intervals, in control conditions (white; $n = 9$, $n = 8$, respectively), in the presence of 200 μM D-APV (black; $n = 5$, $n = 4$, respectively) or in the presence of 50 μM CPCCOEt (gray; $n = 6$). (*E*) LTD induced upon GCL stimulation is still frequency and NMDAR dependent (Ctrl $n = 8$, APV $n = 4$, 60 ms $n = 4$). For *D* and *E*, *, $P < 0.02$; Mann–Whitney U test.

(GCL) (Fig. 1*E*). These results show that the induction of depression depends on the frequency of PF activity.

LTD Induction Requires NMDA Receptor Activation. What determines the PF frequencies able to induce LTD? Because PF activity leads to glutamate release, we investigated whether glutamate receptor activation was involved in selection of activity patterns. At PF-PC synapses, two different types of receptors to glutamate have been reported to play a role in LTD induction: mGluR1 receptors of PCs (27–30) and presynaptic NMDARs of PFs (14).

Although recent studies have shown that PCs of adult mice express functional NMDARs at synapses with climbing fibers (31, 32), functional NMDARs are not present after postnatal day 7 in PCs of juvenile rats (33, 34) (Fig. S2). However, NMDA antagonists prevent LTD induction (14, 24). In previous work, we reported that the activation of presynaptic NMDA receptors present at PF-PC synapses is a permissive condition for LTD induction (14). In Fig. 1*D*, we show that the 5-ms interval protocol failed to induce LTD in the presence of the NMDAR antagonist D-APV ($5.1 \pm 5.7\%$, $n = 5$, $P = 1$) (Fig. S3). When a 1-ms interval protocol was used, D-APV also prevented LTD induction ($-1.2 \pm 7.5\%$, $n = 4$, $P = 0.62$). Similar results were obtained when LTD is induced by alternative induction protocols, that is, by pairing CF and PF activities (Fig. S1) or when the PF input is sparse by stimulating the GCL (Fig. 1*E*). Thus, we confirm that NMDAR activation is an absolute requirement for LTD induction. We then set out to test whether NMDARs are also responsible for the dependence of LTD induction on repetitive, high-frequency activity in PFs.

It could be argued that the need for repetitive activity for LTD induction arises from metabotropic mGluR1 receptor activation. PC mGluR1 activation is known to require repetitive activity of PFs (35, 36), probably because of the perisynaptic location of these receptors (37, 38). Pharmacological and transgenic approaches have shown that mGluR1 receptor activation can contribute to the PC calcium increase necessary for LTD induction (17, 28, 30, 36, 39). However, we show here that LTD can still be induced in the presence of the noncompetitive selective antagonist of mGluR1 receptors, CPCCOEt (Fig. 1*D*) ($25.5 \pm 4.0\%$, $n = 6$, $P < 0.04$, similarly to control: $P = 0.35$, Mann–Whitney U test, see Fig. S3). This may be due to a bypass of the mGluR1 requirement by our experimental pairing protocol (i.e., a robust PC depolarization supplying sufficient Ca via voltage-dependent Ca channels), as shown by others (19, 22, 40). Consistent with this, LTD induced in a sparse set of synapses by placing the stimulation electrode in the GCL is of somehow lesser amplitude (Fig. 1*E*). In these conditions, glutamate buildup after spillover is unlikely (41–44). Therefore, LTD induction depends on NMDAR activation but not on that of mGluRs.

An NR2A-Selective Antagonist Prevents LTD Induction. Because of their slow gating kinetics, NMDA autoreceptors would not be expected to conduct effectively after a single action potential. Instead, repolarization of the PF would cause voltage-dependent Mg block of NMDARs. Conduction of Ca by NMDA autoreceptors should therefore require the relief of Mg block by a second action potential within an interval defined by the residence time of glutamate on the NMDA receptor. This hypothesized mechanism therefore predicts a precise correspondence between the kinetics of glutamate unbinding from the NMDARs and the action potential frequencies that are effective in inducing LTD.

To test this hypothesis, we needed to know the exact deactivation

NEUROSCIENCE

time course of PF NMDARs, but this depended on two unknowns: i) the specific NMDAR subunits expressed by PFs and ii) their kinetics at near physiological temperature. Thus, it is known that the deactivation time constants (which reflect glutamate unbinding) of NMDARs vary from 10s of milliseconds to several seconds, depending on the subunit and temperature (45–47). NMDARs are heterotetramers composed of NR1 and NR2 subunits, the latter being the products of four separate genes (NR2A to D).

As a first step to determining which NR2 subunits contribute to LTD induction, we used two noncompetitive antagonists that discriminate between NR2A- and NR2B-containing receptors: zinc ions (Zn^{2+}) in the nanomolar range specifically antagonize NR2A-containing NMDARs (48) whereas Ro25–6981 (R-(R*,S*)-α-(4-hydroxyphényl)-β-methyl-4-(phenyl-methyl)-1-piperidine propanol), an ifenprodil analog, specifically antagonizes NR2B-containing NMDARs (49, 50). We checked the specificity of these antagonists on recombinant NMDARs expressed in HEK cells (Fig. S4). Zinc ions (300 nM) inhibited NR1+NR2A currents (84.6 ± 3.0% inhibition; $n = 4$) without affecting NR1+NR2B (9.3 ± 7.7%; $n = 4$) or NR1+NR2C (4.5 ± 1.5%; $n = 3$) currents. In the same manner, Ro25–6981 (300 nM) inhibited NR1+NR2B currents (75.9 ± 4.9% inhibition; $n = 4$) without affecting NR1+NR2A (4.3 ± 7.8%; $n = 4$) or NR1+NR2C (−6.7 ± 3.9%; $n = 3$) currents. Neither of these compounds had a significant effect on basal AMPA-mediated fast transmission between PFs and PCs (Fig. S5).

We then set out to test the actions of Zn and Ro25–6981 on LTD induction. In the presence of the NR2A antagonist Zn, the 5-ms interval protocol failed to induce LTD (depression: 4.5 ± 9.2%, $n = 5$, $P = 0.375$) (Fig. 2 *A*, *C*, and *D*). This was significantly different from the control experiment ($P < 0.02$, Mann–Whitney U test) (Fig. 1*C*). In contrast, in the presence of the NR2B antagonist Ro25–6981, the 5-ms interval protocol still induced LTD (24.6 ± 3.4%, $n = 6$, $P < 0.04$) (Fig. 2 *B–D*), not different from the depression in control conditions ($P = 0.48$, Mann–Whitney U test) (Fig. 1 *C*). Therefore, NR2A- but not NR2B-containing NMDARs are required for LTD induction.

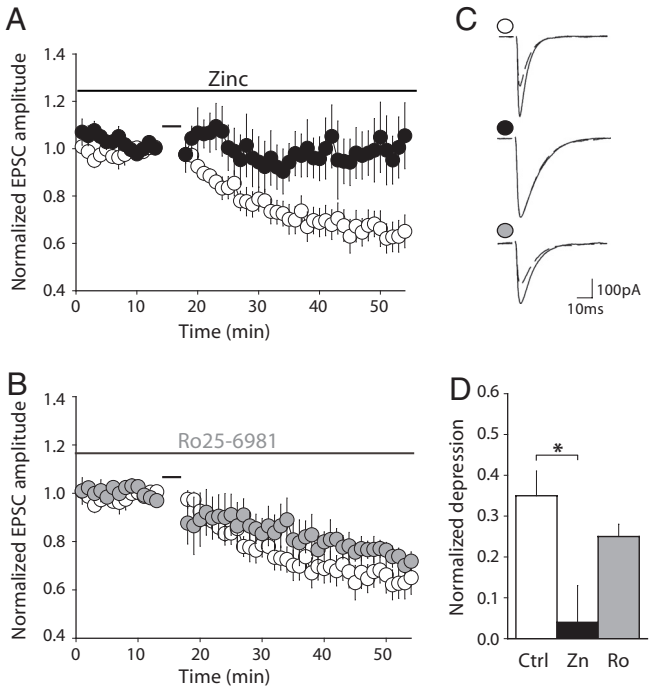

Fig. 2. NR2A- but not NR2B-containing NMDAR are required for LTD induction. (*A*) The NR2A antagonist zinc prevents LTD induction. Time course of the EPSC amplitude in control conditions (white; $n = 9$; same data as in Fig. 1) or in the presence of 300 nM free buffered zinc (black; $n = 5$). In each case, pairing was done with double PF stimuli at a 5-ms interval. (*B*) LTD is still induced in the presence of the NR2B antagonist Ro25–6981. Time course of the EPSC amplitude in control conditions (white; $n = 9$; same data as in Fig. 1) or in the presence of 300 nM Ro25–6981 (gray; $n = 6$). The application of Ro25–6981 started at least 15 min before induction. In each case, pairing was done with double PF stimuli at a 5-ms interval. (*C*) Records from representative experiments in control conditions (*Top*), in 300 nM free zinc (*Middle*) or 300 nM Ro25–6981 (*Bottom*). Traces are averages of 10 sweeps, just before pairing (solid) and 30 min after pairing (dashed). (*D*) Depression induced by pairing with double PF stimuli at a 5-ms interval in control conditions (white; $n = 9$), in 300 nM free zinc (black; $n = 5$) or in 300 nM Ro25–6981 (gray; $n = 6$). *, $P < 0.02$; Mann–Whitney U test.

Parallel Fibers Express Presynaptic NR2A-Containing NMDA Receptors. To test directly for the presence of NMDAR subunits in PFs, we performed immunohistochemistry with antibodies against NMDAR subunits. We filled PCs in acute slices with neurobiotin by the means of a patch pipette. Then we performed immunohistochemistry with an antibody directed against NR2A. No staining was observed on PC dendrites or spines, but punctate staining was observed juxtaposed to PC dendritic spines (50/208 spines) (Fig. 3*A*). This is consistent with labeling of PF varicosities. However, the resolution of optical microscopy is not sufficient to identify unequivocally the element stained. Thus, we decided to use preembedding immuno-electron microscopy (EM) to study the distribution of NMDARs. PF-PC synapses were identified following the morphological criteria described by Palay and Chan-Palay. The peroxidase-amplified immunostaining showed the presence of NR1 (Fig. 3 *B* and *C*), NR2A (Fig. 3 *D* and *E*) and to a lesser extent NR2B subunits on PF boutons. PC spines or glial processes were very rarely stained. The quantification of morphologically identified PF-PC synapses revealed that at least 49% of PF-PC synapses expressed NR1, whereas 23% expressed NR2A and only 10% expressed NR2B (Fig. 3*F*). The subunit identity of the NMDARs shown on PFs by immunohistochemistry fits with the pharmacological profile of the receptors involved in LTD induction.

Subunit-Specific Kinetics of NMDA Receptors Define the PF Frequencies Resulting in Plasticity. Having identified the NMDAR subunits involved in LTD induction, we then measured the deactivation rates of recombinant receptors at near-physiological temperature because subunit-specific kinetic information was only available from experiments carried out at room temperature.

Rapid application of 1 mM glutamate (100-ms steps) to HEK cells expressing recombinant NMDARs induced inward currents as shown in Fig. 4*A*. The recording temperature was 32 °C, as for our synaptic experiments. To focus on the deactivation kinetics of the receptors, currents were normalized to the amplitude at the end of the agonist application (Fig. 4*B*). Deactivation kinetics were several fold faster at 32 °C (same temperature as for LTD experiments) than at room temperature. Values of the decay time constant were extracted by fitting single exponentials. The deactivation time constants τ of NMDARs were 28.6 ± 4.7 ms ($n = 10$), 193.2 ± 14.9 ms ($n = 10$), and 217.6 ± 37.6 ms ($n = 8$) for NR2A−, NR2B−, and NR2C-containing NMDARs, respectively. The relative order of the NR2 subunit deactivation time constants thus remained consistent with that determined at room temperature (45, 46).

A comparison between the dependence of LTD on interspike interval and the deactivation time courses at 32 °C of recombinant NMDAR containing different NR2 subunits is shown in Fig. 4*C*. The magnitude of LTD as a function of PF firing interval fits very closely with the NR1+NR2A deactivation time course and does not fit with those of NR1+NR2B or NR1+NR2C, thus verifying the prediction of a precise temporal correlation between these two processes. We conclude that the presynaptic frequency dependence of LTD induction can be fully accounted for by the presence of NR2A-containing NMDA autoreceptors on PFs.

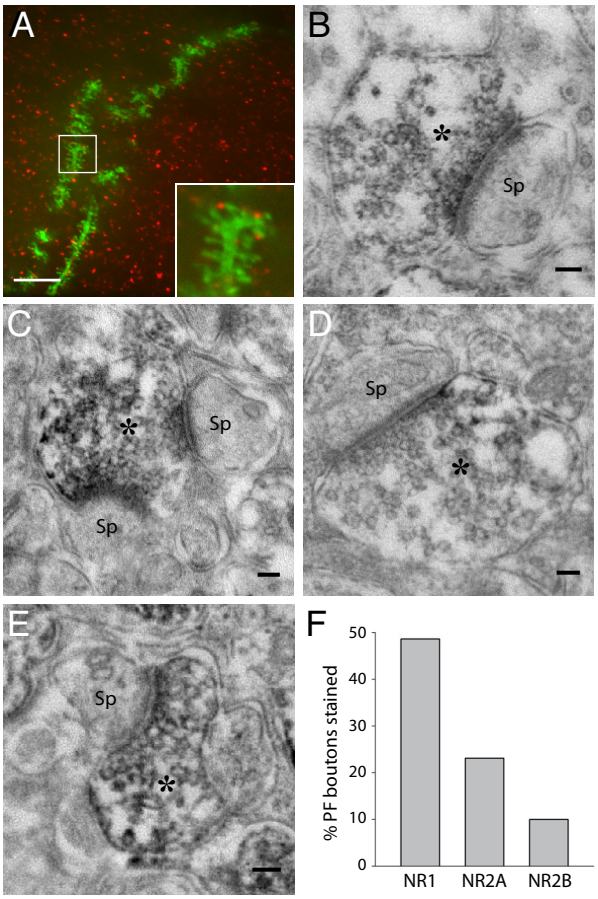

Fig. 3. Immunohistochemistry reveals the presence of NR1, NR2A, and NR2B at presynaptic sites of PF-PC synapses. (*A*) Fluorescence image of a segment of a dendrite in a neurobiotin-filled PC (green) combined with immunohistochemistry against the NR2A subunit of the NMDAR (red) in a coronal slice. (Scale bar: 1 μm.) (*B–E*) Electron microscopy of peroxidase-amplified immunostaining of NMDAR subunits. Note the PF varicosities (*) with synaptic vesicles and the postsynaptic densities of PC spines (Sp). (*B* and *C*) NR1 staining. (*D* and *E*) NR2A staining. (Scale bars, 100 nm.) (*F*) Quantification of peroxidase labeling of PF boutons: 48.6% of the PF boutons in a given region (177/364 PF-PC synapses) were reactive for NR1, 23.1% (63/273 PF-PC synapses) for NR2A, and 10.0% (26/261 PF-PC synapses) for NR2B antibodies.

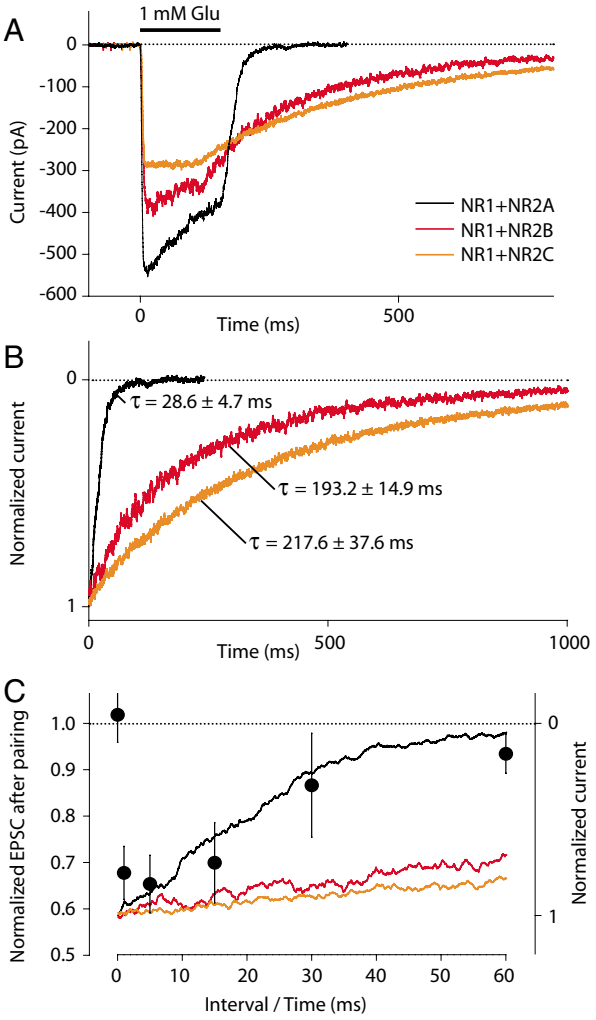

Fig. 4. Deactivation rates of recombinant NMDA receptors at 32 °C. (*A*) NMDAR currents (average of 5–10 consecutive traces) elicited by 100 ms-long applications of L-glutamate (1 mM) in the presence of 100 μM glycine to small lifted HEK-293 cells transfected with different NMDAR subunit DNAs (NR1–1a plus NR2A, NR2B, or NR2C). (*B*) NMDAR currents in *A* normalized to the amplitude at the end of the agonist application. Values of the deactivation time constants (τ_{off}) are mean ± SEM. $n = 10$ for NR1+NR2A and NR1+NR2B; $n = 8$ for NR1+NR2C. (*C*) The range of PF stimulation intervals resulting in LTD fits with the NR1+NR2A deactivation time course. The interval dependence of LTD induction (Fig. 1*C*) is plotted with the deactivation time courses of NMDAR currents (Fig. 4*B*). The start of current decay was aligned with the 0-ms interval for LTD induction and 0 NMDA current was aligned vertically with zero LTD.

Discussion

NMDAR Signaling for LTD Induction Arises from PF Terminals. NMDAR activation (14, 24) and transcellular NO signaling (20–22, 24) are necessary for cerebellar LTD induction. In many systems, NO has been shown to be produced after NMDAR activation (51–54). In the cerebellar cortex, GCs express nNOS (55, 56) and NO signaling is the result of PF activity (21–23, 57).

We show that bursting activity of PFs is necessary for cerebellar LTD induction. The range of PF frequencies capable of inducing LTD indicates that the system behaves as a high-pass filter with a corner frequency ≈40 Hz (Fig. 1).

A heterosynaptic recruitment of glutamate receptors after repetitive activity (44, 58) does not seem to be involved in the requirement for repetitive firing, because LTD can be induced when the input is restricted to a single fiber (GC-PC paired recordings in ref. 14). Furthermore, LTD can be induced in a sparse set of synapses through GCL stimulation (Fig. 1*E*). Thus, the spatial integration of multiple inputs because of spillover of glutamate to neighboring synapses (41, 42) is not necessary.

An alternative hypothesis for the frequency dependence of LTD induction would involve the activation of mGluR1 receptors in PCs. mGluR1 receptors are known to contribute to the Ca signal required for LTD induction (17, 36, 39, 59). However, mGluR1 activation may not be necessary in experimental situations where the Ca entry through voltage-dependent channels in PCs is optimal (60) (Fig. 1 and Fig. S3). Bypass of mGluR1 activation may be achieved when depolarization-induced Ca spikes are present during induction (see *Materials and Methods*). Nevertheless, we cannot exclude the possibility that, in physiological conditions, a requirement for mGluR1 activation may increase the gain for discrimination in favor of repetitive activity patterns. Indeed, LTD is of a smaller amplitude when induced by GCL stimulation (Fig. 1 *E* vs. *D*), an experimental situation where mGluR activation is reduced (43, 44).

Finally, the frequency dependence of LTD induction may originate from the mode of activation of presynaptic NMDARs. In Fig.

NEUROSCIENCE

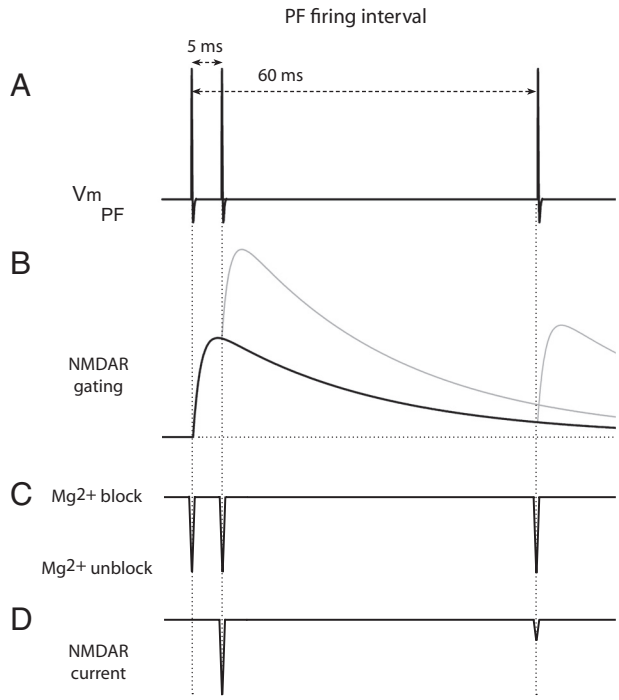

Fig. 5. NMDA autoreceptors as burst detectors. Schematic view of PF membrane potential and associated states of presynaptic NMDARs. (*A*) Time course of the PF membrane potential ($V_{m,\ PF}$) during high or low frequency activity (200 Hz vs. 16.7 Hz). (*B*) Gating of NMDA autoreceptors activated by glutamate released by the action potentials. Receptor kinetics have been extracted from those of recombinant NR1+NR2A receptors measured in Fig. 4 (τ_{on} = 1.4 ms; τ_{off} = 28.6 ms). (*C*) Voltage-dependent Mg block of NMDARs. (*D*) Current flow through NMDARs occurs only when receptors are gated and the Mg block is relieved. The effective interval between two successive PF action potentials for NMDAR conduction is defined by the residence time of glutamate on NMDARs. The first action potential provides the glutamate. By the time the receptor opens, the membrane is repolarized and Mg blocks the channel. The second action potential relieves the Mg block and Ca flows through the channel into the PF terminal only if it arrives while glutamate is still bound to the receptor (200 Hz). If the second action potential arrives after glutamate unbinding (16.7 Hz), little current flows.

5 we present a schematic view of the events leading to autoreceptor opening. First, after a release event, glutamate binds to NMDARs. However, the depolarization associated with the action potential is short, and by the time glutamate binds to the receptor and promotes its opening (61), the Mg block precludes receptor opening. Permeation through NMDARs will only occur if a second action potential is elicited before glutamate dissociates.

This hypothesis makes a precise prediction. The time of residence of glutamate on NMDARs will define the interval of PF firing effective for LTD induction. Because glutamate unbinding is strongly dependent on the subunit composition of the receptors, the time course for effective LTD induction should match the properties of the combination of subunits present in PFs. We have measured the kinetics of different recombinant NMDARs (Fig. 4). Only the kinetics of NR2A-containing NMDARs are compatible with the effective LTD induction interval (Fig. 4*C*). Immunohistochemistry and the pharmacological characterization of LTD reinforce our hypothesis (Figs. 2 and 3).

The existence of NMDARs on PFs has been controversial (24, 13). However, we provide direct evidence for the existence of NMDARs on PFs and for their involvement in LTD induction. Immunoelectron microscopy shows that PFs do express NMDARs (Fig. 3). These receptors are essentially composed of NR1 and NR2A subunits. The presence of NR2A subunits on PFs matches both the pharmacological and the kinetic properties of LTD induction (Figs. 2 and 4). These results strongly support the idea that NMDAR-NOS signaling during LTD takes place directly in PFs. The NMDAR-NOS Ca signaling domain would be independent of that serving transmitter release, because pairing in the presence of APV is unable to induce plasticity (14) (Fig. 1) and NMDAR activation does not affect transmitter release (5). This separation would imply the existence of specific and different molecular scaffoldings for the "release domain" (VDCC and release machinery) and the "plasticity domain" (NMDAR and nNOS).

NMDA Autoreceptors Define the Temporal Properties of the Plasticity Rule. We show that in addition to the well-known detection of the temporal correlation between CF and PF activities, LTD induction at PF-PC synapses also relies on a temporal integration of PF activity: PFs must fire at least twice within a short time window. Interestingly, in previous experiments, we successfully induced LTD at room temperature using pairs of stimuli separated by as much as 60 ms (14). This is in contrast with the narrower timing profile shown here at 32 °C, but is explained by the slower kinetics of NMDAR at lower temperatures (45–47). Indeed, slight changes in experimental temperature may shift the corner frequency for plasticity induction, which is probably somehow higher at 37 °C than the 40 Hz measured here. The onset kinetics of the NMDAR activation might be expected to determine the upper limit of the frequency range resulting in plasticity. However, at physiological temperature, the gating of NMDARs (47) occurs on the same time scale as the absolute refractory period of the PF action potential (26, 62).

The plasticity rule we describe is physiologically relevant because GCs have been shown to be active in vivo at frequencies ranging from a fraction of a Hertz to >1 kHz (25, 26). The firing patterns of GCs depend on mossy fiber (MF) input, intrinsic cellular properties and the cellular circuitry of the GCL. MF input to GCs can itself be composed of bursts (25) and the induction of LTP at MF-GC synapses is able to increase the frequency of GC bursts (63). In addition, the inhibition provided by Golgi cells may shape the relationship between MF input and GC output. In this way, GCL activity may define which inputs may be subject to plasticity at the next synaptic relay.

We propose that the general function of NMDA autoreceptors is the selection of bursting patterns. In cerebellar PFs, the NR2A subunit confers relatively fast kinetics on NMDARs. This high-pass filter defines the GC frequency range that results in plasticity. In other systems, NMDA autoreceptors may be activated by bursting activities at different frequencies depending on the NR2 subunits present. Presynaptic NMDARs located on inhibitory terminals may be activated following different rules. In some cases, such heteroreceptors have been shown to be composed of NR2C or NR2D subunits (64). Because these receptors show little sensitivity to Mg, glutamate binding alone and therefore single action potentials may be sufficient for presynaptic NMDAR activation.

Several studies have highlighted a correlation between presynaptic firing frequency and events triggered by NMDA autoreceptors (15). In the spinal cord, putative presynaptic NMDARs are involved in a high-frequency-induced form of plasticity (4). In the visual cortex, presynaptic NMDARs are necessary for the maintenance of neurotransmission during high-frequency firing (30 Hz) but not during low-frequency firing (0.1 Hz) (8). We propose that the detection of bursting patterns by NMDA autoreceptors constitutes a widespread mechanism. When presynaptic, their biophysical property of coincidence detection is translated into detection of repetitive activity. By imposing a temporal integration mechanism, NMDA autoreceptors implement a plasticity rule that depends on the temporal structure of presynaptic action potential trains, further extending the richness and complexity of synaptic plasticity rules in the brain.

Materials and Methods

Electrophysiology. Animal experimentation complied with French, European and National Institutes of Health guidelines. Experiments were performed on transverse cerebellar acute slices (300 μm) of rats (17- to 24-day-old). See detailed electrophysiological methods in *SI Text*.

Immunohistochemistry. Antibody specificity was established by Western blot (WB) analysis on extracts from *Xenopus* oocytes expressing recombinant NMDARs. We also characterized the native NMDAR subunits in cerebellar membrane preparations (Fig. S6). See detailed immunohistochemical methods in *SI Text*.

ACKNOWLEDGMENTS. We thank P. Rostaing for teaching us EM; A. Le Goff and M. Gielen for WB; and P. Ascher, A. Marty, S. Dieudonné, and P. Paoletti for helpful comments. This work was supported by Ecole Normale Supérieure, Centre National de la Recherche Scientifique, Agence Nationale de la Recherches (ANR), ANR-05-NEUR-030, ANR-08-BLAN-0023, ANR-08-SYSC-005-01 (to B.B.), and ANR-06-BLAN-0029 (to M.C.).

1. Nowak L, Bregestovski P, Ascher P, Herbet A, Prochiantz A (1984) Magnesium gates glutamate-activated channels in mouse central neurones. *Nature* 307:462–465.
2. Mayer ML, Westbrook GL, Guthrie PB (1984) Voltage-dependent block by Mg2+ of NMDA responses in spinal cord neurones. *Nature* 309:261–263.
3. Berretta N, Jones RS (1996) Tonic facilitation of glutamate release by presynaptic N-methyl-D-aspartate autoreceptors in the entorhinal cortex. *Neuroscience* 75:339–344.
4. Marvizon JC, Martinez V, Grady EF, Bunnett NW, Mayer EA (1997) Neurokinin 1 receptor internalization in spinal cord slices induced by dorsal root stimulation is mediated by NMDA receptors. *J Neurosci* 17:8129–8136.
5. Casado M, Dieudonne S, Ascher P (2000) Presynaptic N-methyl-D-aspartate receptors at the parallel fiber-Purkinje cell synapse. *Proc Natl Acad Sci USA* 97:11593–11597.
6. Woodhall G, Evans DI, Cunningham MO, Jones RS (2001) NR2B-containing NMDA autoreceptors at synapses on entorhinal cortical neurons. *J Neurophysiol* 86:1644–1651.
7. Humeau Y, Shaban H, Bissiere S, Luthi A (2003) Presynaptic induction of heterosynaptic associative plasticity in the mammalian brain. *Nature* 426:841–845.
8. Sjostrom PJ, Turrigiano GG, Nelson SB (2003) Neocortical LTD via coincident activation of presynaptic NMDA and cannabinoid receptors. *Neuron* 39:641–654.
9. Suarez LM, et al. (2005) Presynaptic NMDA autoreceptors facilitate axon excitability: A new molecular target for the anticonvulsant gabapentin. *Eur J Neurosci* 21:197–209.
10. Glitsch M, Marty A (1999) Presynaptic effects of NMDA in cerebellar Purkinje cells and interneurons. *J Neurosci* 19:511–519.
11. Duguid IC, Smart TG (2004) Retrograde activation of presynaptic NMDA receptors enhances GABA release at cerebellar interneuron-Purkinje cell synapses. *Nat Neurosci* 7:525–533.
12. Lien CC, Mu Y, Vargas-Caballero M, Poo MM (2006) Visual stimuli-induced LTD of GABAergic synapses mediated by presynaptic NMDA receptors. *Nat Neurosci* 9:372–380.
13. Christie JM, Jahr CE (2008) Dendritic NMDA receptors activate axonal calcium channels. *Neuron* 60:298–307.
14. Casado M, Isope P, Ascher P (2002) Involvement of presynaptic N-methyl-D-aspartate receptors in cerebellar long-term depression. *Neuron* 33:123–130.
15. Duguid I, Sjostrom PJ (2006) Novel presynaptic mechanisms for coincidence detection in synaptic plasticity. *Curr Opin Neurobiol* 16:312–322.
16. Ito M, Kano M (1982) Long-lasting depression of parallel fiber-Purkinje cell transmission induced by conjunctive stimulation of parallel fibers and climbing fibers in the cerebellar cortex. *Neurosci Lett* 33:253–258.
17. Wang YT, Linden DJ (2000) Expression of cerebellar long-term depression requires postsynaptic clathrin-mediated endocytosis. *Neuron* 25:635–647.
18. Xia J, Chung HJ, Wihler C, Huganir RL, Linden DJ (2000) Cerebellar long-term depression requires PKC-regulated interactions between GluR2/3 and PDZ domain-containing proteins. *Neuron* 28:499–510.
19. Konnerth A, Dreessen J, Augustine GJ (1992) Brief dendritic calcium signals initiate long-lasting synaptic depression in cerebellar Purkinje cells. *Proc Natl Acad Sci USA* 89:7051–7055.
20. Ito M, Karachot L (1990) Messengers mediating long-term desensitization in cerebellar Purkinje cells. *Neuroreport* 1:129–132.
21. Lev-Ram V, Makings LR, Keitz PF, Kao JP, Tsien RY (1995) Long-term depression in cerebellar Purkinje neurons results from coincidence of nitric oxide and depolarization-induced Ca2+ transients. *Neuron* 15:407–415.
22. Lev-Ram V, Jiang T, Wood J, Lawrence DS, Tsien RY (1997) Synergies and coincidence requirements between NO, cGMP, and Ca2+ in the induction of cerebellar long-term depression. *Neuron* 18:1025–1038.
23. Shibuki K, Kimura S (1997) Dynamic properties of nitric oxide release from parallel fibres in rat cerebellar slices. *J Physiol* 498:443–452.
24. Shin JH, Linden DJ (2005) An NMDA receptor/nitric oxide cascade is involved in cerebellar LTD but is not localized to the parallel fiber terminal. *J Neurophysiol* 94:4281–4289.
25. Chadderton P, Margrie TW, Hausser M (2004) Integration of quanta in cerebellar granule cells during sensory processing. *Nature* 428:856–860.
26. Jorntell H, Ekerot CF (2006) Properties of somatosensory synaptic integration in cerebellar granule cells in vivo. *J Neurosci* 26:11786–11797.
27. Daniel H, Hemart N, Jaillard D, Crepel F (1992) Coactivation of metabotropic glutamate receptors and of voltage-gated calcium channels induces long-term depression in cerebellar Purkinje cells in vitro. *Exp Brain Res* 90:327–331.
28. Aiba A, et al. (1994) Deficient cerebellar long-term depression and impaired motor learning in mGluR1 mutant mice. *Cell* 79:377–388.
29. Shigemoto R, Abe T, Nomura S, Nakanishi S, Hirano T (1994) Antibodies inactivating mGluR1 metabotropic glutamate receptor block long-term depression in cultured Purkinje cells. *Neuron* 12:1245–1255.
30. Conquet F, et al. (1994) Motor deficit and impairment of synaptic plasticity in mice lacking mGluR1. *Nature* 372:237–243.
31. Piochon C, et al. (2007) NMDA receptor contribution to the climbing fiber response in the adult mouse Purkinje cell. *J Neurosci* 27:10797–10809.
32. Renzi M, Farrant M, Cull-Candy SG (2007) Climbing-fibre activation of NMDA receptors in Purkinje cells of adult mice. *J Physiol* 585:91–101.
33. Rosenmund C, Legendre P, Westbrook GL (1992) Expression of NMDA channels on cerebellar Purkinje cells acutely dissociated from newborn rats. *J Neurophysiol* 68:1901–1905.
34. Hausser M, Roth A (1997) Dendritic and somatic glutamate receptor channels in rat cerebellar Purkinje cells. *J Physiol* 501:77–95.
35. Batchelor AM, Garthwaite J (1993) Novel synaptic potentials in cerebellar Purkinje cells: Probable mediation by metabotropic glutamate receptors. *Neuropharmacology* 32:11–20.
36. Takechi H, Eilers J, Konnerth A (1998) A new class of synaptic response involving calcium release in dendritic spines. *Nature* 396:757–760.
37. Lujan R, Roberts JD, Shigemoto R, Ohishi H, Somogyi P (1997) Differential plasma membrane distribution of metabotropic glutamate receptors mGluR1 alpha, mGluR2 and mGluR5, relative to neurotransmitter release sites. *J Chem Neuroanat* 13:219–241.
38. Baude A, et al. (1993) The metabotropic glutamate receptor (mGluR1α) is concentrated at perisynaptic membrane of neuronal subpopulations as detected by immunogold reaction. *Neuron* 11:771–787.
39. Miyata M, et al. (2000) Local calcium release in dendritic spines required for long-term synaptic depression. *Neuron* 28:233–244.
40. Hemart N, Daniel H, Jaillard D, Crepel F (1995) Receptors and second messengers involved in long-term depression in rat cerebellar slices in vitro: A reappraisal. *Eur J Neurosci* 7:45–53.
41. Barbour B, Keller BU, Llano I, Marty A (1994) Prolonged presence of glutamate during excitatory synaptic transmission to cerebellar Purkinje cells. *Neuron* 12:1331–1343.
42. Barbour B (2001) An evaluation of synapse independence. *J Neurosci* 21:7969–7984.
43. Marcaggi P, Attwell D (2005) Endocannabinoid signaling depends on the spatial pattern of synapse activation. *Nat Neurosci* 8:776–781.
44. Marcaggi P, Attwell D (2007) Short- and long-term depression of rat cerebellar parallel fibre synaptic transmission mediated by synaptic crosstalk. *J Physiol* 578:545–550.
45. Monyer H, Burnashev N, Laurie DJ, Sakmann B, Seeburg PH (1994) Developmental and regional expression in the rat brain and functional properties of four NMDA receptors. *Neuron* 12:529–540.
46. Vicini S, et al. (1998) Functional and pharmacological differences between recombinant N-methyl-D-aspartate receptors. *J Neurophysiol* 79:555–566.
47. Chen N, Ren J, Raymond LA, Murphy TH (2001) Changes in agonist concentration dependence that are a function of duration of exposure suggest N-methyl-D-aspartate receptor nonsaturation during synaptic stimulation. *Mol Pharmacol* 59:212–219.
48. Paoletti P, Ascher P, Neyton J (1997) High-affinity zinc inhibition of NMDA NR1-NR2A receptors. *J Neurosci* 17:5711–5725.
49. Fischer G, et al. (1997) Ro 25–6981, a highly potent and selective blocker of N-methyl-D-aspartate receptors containing the NR2B subunit. Characterization in vitro. *J Pharmacol Exp Ther* 283:1285–1292.
50. Malherbe P, et al. (2003) Identification of critical residues in the amino terminal domain of the human NR2B subunit involved in the RO 25–6981 binding pocket. *J Pharmacol Exp Ther* 307:897–905.
51. East SJ, Garthwaite J (1991) NMDA receptor activation in rat hippocampus induces cyclic GMP formation through the L-arginine-nitric oxide pathway. *Neurosci Lett* 123:17–19.
52. Dickie BG, Lewis MJ, Davies JA (1992) NMDA-induced release of nitric oxide potentiates aspartate overflow from cerebellar slices. *Neurosci Lett* 138:145–148.
53. Sattler R, et al. (1999) Specific coupling of NMDA receptor activation to nitric oxide neurotoxicity by PSD-95 protein. *Science* 284:1845–1848.
54. Christopherson KS, Hillier BJ, Lim WA, Bredt DS (1999) PSD-95 assembles a ternary complex with the N-methyl-D-aspartic acid receptor and a bivalent neuronal NO synthase PDZ domain. *J Biol Chem* 274:27467–27473.
55. Crepel F, et al. (1994) Cellular locus of the nitric oxide-synthase involved in cerebellar long-term depression induced by high external potassium concentration. *Neuropharmacology* 33:1399–1405.
56. Black SM, et al. (1995) Expression of neuronal nitric oxide synthase corresponds to regions of selective vulnerability to hypoxia-ischaemia in the developing rat brain. *Neurobiol Dis* 2:145–155.
57. Namiki S, Kakizawa S, Hirose K, Iino M (2005) NO signalling decodes frequency of neuronal activity and generates synapse-specific plasticity in mouse cerebellum. *J Physiol* 566:849–863.
58. Hartell NA (1996) Strong activation of parallel fibers produces localized calcium transients and a form of LTD that spreads to distant synapses. *Neuron* 16:601–610.
59. Finch EA, Augustine GJ (1998) Local calcium signalling by inositol-1,4,5-trisphosphate in Purkinje cell dendrites. *Nature* 396:753–756.
60. Crepel F, Jaillard D (1991) Pairing of pre- and postsynaptic activities in cerebellar Purkinje cells induces long-term changes in synaptic efficacy in vitro. *J Physiol* 432:123–141.
61. Kampa BM, Clements J, Jonas P, Stuart GJ (2004) Kinetics of Mg2+ unblock of NMDA receptors: Implications for spike-timing dependent synaptic plasticity. *J Physiol* 556:337–345.
62. Isope P, Barbour B (2002) Properties of unitary granule cell–>Purkinje cell synapses in adult rat cerebellar slices. *J Neurosci* 22:9668–9678.
63. Nieus T, et al. (2006) LTP regulates burst initiation and frequency at mossy fiber-granule cell synapses of rat cerebellum: Experimental observations and theoretical predictions. *J Neurophysiol* 95:686–699.
64. Binshtok AM, Fleidervish IA, Sprengel R, Gutnick MJ (2006) NMDA receptors in layer 4 spiny stellate cells of the mouse barrel cortex contain the NR2C subunit. *J Neurosci* 26:708–715.